



Mango (*Mangifera indica*) seeds and peel-derived hydrocolloids: Gelling ability and emulsion stabilization

Ronald Marsiglia-Fuentes^a, José M. Franco^b, Luis A. García-Zapateiro^{a,*}

^a Research Group in Complex Fluid Engineering and Food Rheology (IFCRA) University of Cartagena, Faculty of Engineering, Department of Food Engineering, Consulate Avenue, St. 30 No. 48-152, Cartagena, Bolívar, Colombia

^b Pro2TecS – Chemical Process and Product Technology Research Centre, Dept. Ingeniería Química, ETSI, Campus de “El Carmen”, Universidad de Huelva, Huelva 21071, Spain

ARTICLE INFO

Keywords:
Byproducts
Emulsions
Hydrocolloids
Mango (*Mangifera indica*)
Rheology

ABSTRACT

Mango is a tropical fruit that is consumed worldwide and is distinguished by its sweet and juicy flesh. Unfortunately, the peels and seeds of mango fruit are often discarded despite the fact that they contain compounds that can be valorized for certain applications. In this study, a physicochemical and hydrodynamic characterization of hydrocolloids extracted from the peel and seeds of mango fruit was performed and the impact on the microstructure and rheological behavior of derived gels, as well as the ability to form emulsions, were analyzed. The physicochemical parameters and proximate compositions of the different samples showed that the hydrocolloids extracted from the seeds are rich in proteins whereas those from the peel are rich in carbohydrates. The molecular weights calculated from the hydrodynamic characterization (M_w) are 101515 g/mol and 102,580 g/mol for hydrocolloids extracted from the peel and seeds, respectively. Dispersions of these hydrocolloids in water produced hydrogels upon heating, which exhibited a shear thinning response that can be described by the Williamson model. The ability of these hydrocolloids to form thermally-induced strong gels was monitored and analyzed by means of curing tests. Throughout thermal treatments, the storage modulus showed a significant increase, especially at concentrations greater than 2.5 wt%. Mango seeds and peel-derived hydrocolloids are also able to stabilize o/w emulsions. Derived emulsions showed D_{50} mean diameters and zeta potential values (ζ) in the ranges from 10.04 to 82.52 μm and from -17.63 to -11.12 mV, respectively. On the basis of the observed rheological behavior of hydrogels and emulsion-forming ability, the hydrocolloids derived from mango seeds and peels possess suitable characteristics to be potentially implemented in diverse food matrices, offering functional and nutritional benefits to final consumer products.

1. Introduction

According to Punia Bangar et al., (2021), mango (*Mangifera indica*) is the most economically important fruit of the Anacardiaceae family (cashew or poison ivy family) and a mass consumption food for the inhabitants of the tropics, mainly its pulp. This can be processed into juices, nectars, drinks, jams (Ke et al., 2022), fruit cheese or eaten alone or with cream as a dessert; it is also used in puddings, bakery fillings and fruit dishes for children (Vergara-Valencia et al., 2007), to make ice creams and yoghurts (Pereira et al., 2021), or introduced as a flavouring ingredient in the food industry (Marçal and Pintado, 2021).

In general, biopolymeric fractions derived from plants and fruits are considered sustainable alternatives that are increasingly used as

renewable raw materials to develop environmentally friendly products (Borah et al., 2020a; Chignola et al., 2022). In the development of new food products, hydrocolloids are often used to impart certain desired properties, such as low-fat or fat-free dairy products (Salvador and Fiszman, 1998; Y. Zhu et al., 2019). Hydrocolloids comprise a variety of long-chain polymers, mainly proteins and polysaccharides, which are employed in the food industry to alter the physical characteristics of liquids. They can form gels or act as thickening, emulsifying, coating, or stabilizing agents (Dickinson, 2003; Phillips and Williams, 2009). Nowadays, the production and application of cost-effective, environmentally sustainable, safe biodegradable hydrocolloids that impart superior physicochemical and nutritional attributes are a challenging goal. With this aim, numerous extraction sources and procedures have been

* Corresponding author.

E-mail address: lgarciaz@unicartagena.edu.co (L.A. García-Zapateiro).

<https://doi.org/10.1016/j.fbp.2024.05.020>

Received 8 February 2024; Received in revised form 17 May 2024; Accepted 31 May 2024

Available online 1 June 2024

0960-3085/© 2024 The Author(s). Published by Elsevier Ltd on behalf of Institution of Chemical Engineers. This is an open access article under the CC BY-NC-ND license (<http://creativecommons.org/licenses/by-nc-nd/4.0/>).

investigated (Liu et al., 2018a), including algae, seeds, fruits and plant exudates (Borah et al., 2020b; Naji-Tabasi and Razavi, 2017). For instance, hydrocolloids extracted from plant materials such as pumpkin peel and seeds have been used to develop new food products such as papaya jam (Martínez et al., 2021) and natural yoghurts (Rojas-torres et al., 2021) whilst *Dioscorea rotundata* hydrocolloids have also been used in the development of low-fat mayonnaise (Rojas-Martin et al., 2023). The effect of these hydrocolloids on the physico-chemical, microstructural and rheological properties at different addition levels has been evaluated.

The rheological properties of hydrocolloids obtained from plant and fruit extracts are of great interest to researchers and commercially relevant in a wide range of fields (De et al., 2020; Farahmandfar and Naji-Tabasi, 2020; Jones et al., 2022; Liu et al., 2018b; Wei et al., 2021). These biopolymers are generally of great importance in the food, pharmaceutical, textile and cosmetic industries, among others (Gupta et al., 2022), due to their ability to modify the rheological characteristics of aqueous systems once dissolved or properly dispersed, acting as gelling agents (Cortez-Trejo et al., 2022), thickeners (Blok et al., 2023), emulsifiers and stabilizers (Cao et al., 2023). A comprehensive rheological characterization is essential to assess the flow and deformation of liquid and semisolid food products (Wang and Selomulya, 2022). This scientific discipline is well suited to study foods with complex compositions or testing food processes such as sol-gel transitions, starch sticking, protein denaturation, and fat melting, among others. For instance, the rheological evaluation of emulgel production with passion fruit peel pectin has been applied to establish the concentrations that make the product more stable, where the yield stress, elastic deformation, and elastic modulus increase when converting an emulsion into an emulgel (Kavya et al., 2023). Dynamic viscoelastic rheological testing has also been used to determine the characteristics of solutions formulated from sesame hydrocolloids to establish the gelling ability at different temperatures and frequency ranges (Lastra-Ripoll et al., 2022a).

The hypothesis is that hydrocolloids derived from these residues can be used as gelling and emulsifying agents in food systems, similarly to other well-known hydrocolloids, such as guar gum. Unlike traditional hydrocolloids like guar gum, which are often derived from specific cultivated crops, the utilization of mango waste offers several advantages. Initially, extracting hydrocolloids from mango waste promotes resource efficiency by utilizing abundant byproducts of mango processing industries that would otherwise be considered waste and discarded. This approach reduces the need to rely solely on agricultural resources for hydrocolloid production, thus conserving resources and minimizing environmental impact. Also, the utilization of waste materials for hydrocolloid extraction can potentially reduce production costs compared to using commercially available hydrocolloids like guar gum. By repurposing mango waste, this approach supports with the principles of circular economy by turning waste into valuable resources (de Lourdes García-Magaña et al., 2013).

The main objective of this study was to investigate the physico-chemical, hydrodynamic, and rheological properties of hydrocolloid systems derived from mango (*Mangifera indica*) peel and seed extracts and their ability to stabilize emulsions. The focus was on understanding the distinctive characteristics of these hydrocolloids and their potential applications in food formulations, particularly in the context of hydrogels and emulsion development. By studying the hydrodynamic properties and rheological behavior of these hydrocolloids, this research aims to provide valuable insights into the use of these hydrocolloids as gelling and stabilizing agents in food emulsions, which can significantly impact the texture, stability, and overall quality of food products.

2. Materials and methods

2.1. Materials

Mango (*Mangifera indica*) var. Tommy was purchased in the mature organoleptic stage on the local market of Cartagena de Indias (Colombia). The raw materials were sterilized by immersion in a sodium hypochlorite solution (100 ppm) for 15 min at 30 °C. The peel, pulp, and seeds were then removed manually. The reduction in particle size was carried out in an Ika MF 10.2 mill equipped with a sieve to achieve a particle size of less than 250 µm after freezing the pulp, seeds, and peel for 72 h in a 1.5-liter Lab-conco Freezone benchtop unit.

2.2. Chemical reagents

Buffer solutions (boric acid/potassium chloride/sodium hydroxide), sodium azide, and phenolphthalein were purchased from Sigma-Aldrich (St. Louis, MO). Analytical-grade chemicals, including ethanol, glacial acetic acid, hexane (99.5 %) and sulfuric acid (96 %) were purchased from Panreac (Barcelona, Spain).

2.3. Hydrocolloid extraction process

Hydrocolloid extraction from the peel and seeds was carried out according to the methods described in a previous study (Marsiglia-Fuentes et al., 2022), evaluating the effects of pH of solubilization (3 and 10) and using a 1:8 w/w solid:water ratio (see Table 1). First, the raw materials (peel and seeds) were dispersed in distilled water at 80 °C for 4 h. Initially, the pH value (3 and 10) of these solutions was adjusted using acetic acid and NaOH. The mixture was then subjected to centrifugation at 4000 rpm for 15 min to separate the liquid phase. Subsequently, the liquid phase was combined with ethanol in a 1:1 v/v ratio and left to interact for 3 h at a temperature of 2 °C to facilitate the precipitation of the hydrocolloids. Subsequently, the resulting mixture was subjected to another round of centrifugation (4000 rpm) and the resulting precipitate was collected and subjected to freeze-drying at -50 °C and 0.02 Pa for 72 h. The extraction yield of hydrocolloids (g hydrocolloid extract/g mango part × 100) was calculated in the four resulting extract powders: peel and seed extracts at pH 3 and 10 (HP₃, HS₃, HP₁₀ and HS₁₀), respectively.

2.4. Chemical characterization

Proximal composition of the hydrocolloids, including moisture, lipids, ash, and protein content, were determined following the guidelines specified in the Association of Official Analytical Chemists (AOAC) Standard Methods (Horwitz, 2010) 926.08, 972.28, 935.42, and 926.123, respectively. Titratable acidity was assessed by alkalimetric titration with 0.1 N NaOH using phenolphthalein as an indicator (AOAC No. 967.21). pH measurements were made using a pre-calibrated Mettler Toledo AG SG2 digital potentiometer, following the method described in AOAC 942.05. Furthermore, Fourier transform infrared (FTIR) spectroscopy was used to identify the main functional groups in each sample. FTIR spectra were obtained in a FT/IR - 4100 spectrometer (JASCO, Spain), from 500 to 4000 cm⁻¹, with a 4 cm⁻¹ resolution and 32 average

Table 1
Hydrocolloids extraction conditions from peel and seed of mango (*Mangifera indica*) var. Tommy.

Sample code	parts of Mango fruit	pH	solid:water ratio (w/w)	time (h)	Yield (%)
HP ₃	Peel	3	1:8	4	7.64
HP ₁₀	Peel	10	1:8	4	7.66
HS ₃	Seed	3	1:8	4	6.45
HS ₁₀	Seed	10	1:8	4	8.22

scans.

2.5. Intrinsic viscosity and molecular weight determination

To determine the intrinsic viscosity of hydrocolloids, a 0.5 % w/v solution of the sample was prepared in a screw cap under magnetic stirring for 4 h or until complete dissolution and allowed to stand for 20 min to eliminate bubbles formed during homogenization. A capillary-type kinematic viscometer (DIN 51562 part 1 - ISO 3105 - UNE 400313) with a constant of 0.087437 cSt/s, equipped with a thermostatic bath at 25 °C was used to determine, the relative (Eq. (1)), specific (Eq. (2)), and reduced (Eq. (3)) viscosities of the solvent and corresponding solutions pouring times as follows:

$$\eta_{rel} = \frac{t}{t_0} \quad (1)$$

$$\eta_{sp} = \frac{t - t_0}{t_0} \quad (2)$$

$$\eta_{red} = \frac{\eta_{sp}}{C} \quad (3)$$

where t_0 and t correspond to the pouring times of the solvent and each solution.

These viscosities are related to intrinsic viscosity or limit viscosity index, which can be calculated using single-point methods such as that of Solomon-Ciuta (da Costa et al., 2017; Pamies et al., 2008), expressed in Eq. (4). Once the intrinsic viscosity is known, the molecular weight was determined using the Mark-Houwink-Sakurada (MHS) equation (Eq. (5)), where the $K_{[\eta]}$ and a constant values were taken for the studies performed with similar systems, i.e. guar gum and galactomannans in distilled water ($K_{[\eta]} = 5.13 \times 10^{-4} \text{ g.mL}^{-1}$, $a = 0.72$) (Beer et al., 1999; Picout and Ross-Murphy, 2007).

$$[\eta] = \frac{[2(\eta_{sp} - \ln \eta_{rel})]^{1/2} - 1}{C} \quad (4)$$

$$[\eta] = K_{[\eta]} * Mw^a \quad (5)$$

2.6. Scanning electron microscopy (SEM)

Scanning electron microscopy (SEM) observations were carried out using a JEOL JSM 5950 LV equipment, by applying a 25 Pa high vacuum and 15 kv electric current to microstructurally analyze the formulations obtained by dispersing the hydrocolloids in water. The samples were initially freeze dried and coated with a thin layer of gold for observations at 300x and 600x magnification (Bhusari et al., 2014; Rayo et al., 2015).

2.7. Preparation of the hydrocolloid system

Based on the yield, chemical characterization, and valorization of the mango waste products (seeds and peel), different hydrocolloid formulations were prepared at different concentrations using samples extracted at pH 3 by applying a heat treatment and magnetic agitation, without variation in pH. The dispersions of hydrocolloids in deionized water at different concentrations (see Table 2) were heated to 90 °C under stirring, centrifuged to remove air bubbles, and cooled at 5 °C for 24 h, according to the methodology proposed by Han et al. (2022). At the same time, 0.1 % sodium chloride (NaCl) was added with saccharose to the hydrocolloidal system to promote gel formation.

2.8. Rheological measurements

2.8.1. Steady-state viscous flow

A plate-plate geometry (35 mm diameter, 1 mm gap) was used in a

Table 2

Formulation of hydrocolloid systems from the valorized fraction of the mango peel and seed.

Sample code	Hydrocolloids (%)	Deionized water (mL)	Salt NaCl (%)	Saccharose C ₁₂ H ₂₂ O ₁₁ (%)
HP ₃ -1	1	30	0.1	0.1
HP ₃ -2.5	2.5	30	0.1	0.1
HP ₃ -5	5	30	0.1	0.1
HS ₃ -1	1	30	0.1	0.1
HS ₃ -2.5	2.5	30	0.1	0.1
HS ₃ -5	5	30	0.1	0.1
*C (Guar gum)	1	30	0.1	0.1

HP₃: Hydrocolloids formulated from peel extracts at pH 3; HS₃: Hydrocolloids formulated from seed extracts at pH 3; *C: Control.

controlled stress rheometer (Haake MARS 60, Thermo-Scientific, Germany) to characterize the rheological properties of hydrocolloid formulations. The procedures were carried out according to the methodology described previously (Marsiglia et al., 2021). Before the rheological test for each sample was conducted, a 10-min equilibration period was implemented to ensure a consistent sample relaxation history. In general, the temperature during the test was maintained at 25 °C using a Peltier device.

Steady-state viscous flow tests were performed over a shear rate range from 10^{-3} to 10^3 s^{-1} . The viscoelastic responses were evaluated by small-amplitude oscillatory shear (SAOS) tests. Frequency sweeps from 0.02 to 100 rad/s were performed within the linear viscoelasticity range. Previously, to determine the extension of the linear viscoelasticity regime, stress sweeps were performed at a frequency of 1 Hz with an increasing sequence of stresses from 10^{-3} to 10^3 Pa .

2.8.2. Curing test

Curing tests were conducted to monitor the rheological properties of gelling solutions prepared with hydrocolloids without heating; in this case, heat treatments were applied at the up / down temperature ramp. To prevent breakage of the gels, the maximum temperature was set at 70 °C. Temperature sweeps were performed from 25 °C to 70 °C at 4 °C/min and 1 rad/s, maintaining the maximum temperature for 20 min, and subsequently decreasing the temperature from 70 °C to 25 °C at 4 °C/min. Then a frequency sweep was conducted at 25 °C to study the variation of the storage (G') and loss (G'') moduli of the heat-induced gels.

2.9. Emulsion preparation and characterization

The emulsions were prepared by dispersing 10 % sunflower oil in 90 % aqueous solutions incorporating 1.25 wt% of the HP₁₀, HP₃, HS₁₀ and HS₃ samples over the total emulsion, without adding any other emulsifier or stabilizing agent. Droplet size distribution (DSD) measurements were performed with a Mastersizer 2000 laser diffractometer (Malvern Instruments, Worcestershire, UK). The samples were diluted in deionized water at 2000 rpm until an obscuration rate of 10 % was achieved. Mie's theory was applied with a refractive index of 1.52 and an absorption of 0.1 for each treatment (presumably a reference material). Three samples of each formulation were measured in quintuplicate. Additionally, the ζ -potential was determined at 25 °C using a Zetasizer nano-Z device (Malvern Instruments, Worcestershire, UK). The mathematical model of Smoluchowsky was used to convert electrophoretic mobility measurements into ζ -potential values (Sánchez-González et al., 2009).

2.10. Statistical analysis

ANOVA (unidirectional) was used to analyze the data using SPSS

software (version 17.2 for Windows) to find statistically significant differences ($p < 0.05$) between samples.

3. Results and discussion

3.1. Physicochemical parameters and proximal composition

The selected physicochemical parameters and the proximal composition of the hydrocolloids extracted from the waste materials of the mango Tommy variety, ie, the peel and seeds, at pHs 3 (HP₃ and HS₃) and 10 (HP₁₀ and HS₁₀) are shown in Table 3. Depending on the solubilization settings, the sample has variable pH values ($p < 0.05$). HP₃ and HS₃ had pH values of 4.35 and 4.56, while HP₁₀ and HS₁₀ had pH values of 8.25 and 8.16, respectively. The addition of a neutral solvent, a substance such as ethanol, during the precipitation stage causes an increase or decrease in the pH value with respect to the pH imposed in extraction (Petrucci et al., 2017). The moisture and ash contents of the hydrocolloids showed no significant or slight differences. However, the fat content of the HS₃ (16.85 %) and HS₁₀ samples (17.33 %) are significantly higher ($p < 0.05$) than those found in the HP₃ samples (2.86 %) and HP₁₀ (2.75 %). Furthermore, the carbohydrate content varied significantly between the samples, with HP₃ and HP₁₀ showing values around 75.15 % and 76.16 % respectively, while HS₃ and HS₁₀ had values of 33.42 % and 32.45 %. This disparity in the carbohydrate content of hydrocolloids can be attributed to the composition of the raw material used, as reported for hydrocolloids derived from sesame, guar gum, and tortuosa gum exudate (Lastra-Ripoll et al., 2022b; M. Martínez et al., 2015), typically peel having a high content of starches and other polysaccharides. The protein content also showed a significant difference between samples HS₃ (33.42 %) and HS₁₀ (32.45 %), and samples HP₃ (0.38 %) and HP₁₀ (0.35 %). This disparity in protein and polysaccharide contents must be attributed to the inherent composition of the seeds and peels and the coprecipitation of proteins and polysaccharides from the seeds and peels when the supernatant was mixed with ethanol during the extraction process (H. Zhu et al., 2023).

In Fig. 1 shows the FTIR spectra of the hydrocolloids obtained, the bands at 3300 cm⁻¹ in all samples are attributed to O–H stretching vibration, indicating intramolecular and intermolecular hydrogen interactions. Vibrations of symmetrical C–H stretching of the lipid extension are observed in the 2850 cm⁻¹ band for HS₃ and HS₁₀. The band at 1750 cm⁻¹ is associated to the stretching vibration of the C–O bond in non-ionic carboxyl groups or their ester acids (–COOH, –COOCH₃) in all samples (Eitex, 2017). The typical bands at 1400 cm⁻¹ in HP₃ and HP₁₀ are assigned to the symmetric and asymmetric stretching vibrations of –COO uronic acids (Razavi et al., 2014). The bands around 1020 cm⁻¹ are attributed to the stretching vibrations of

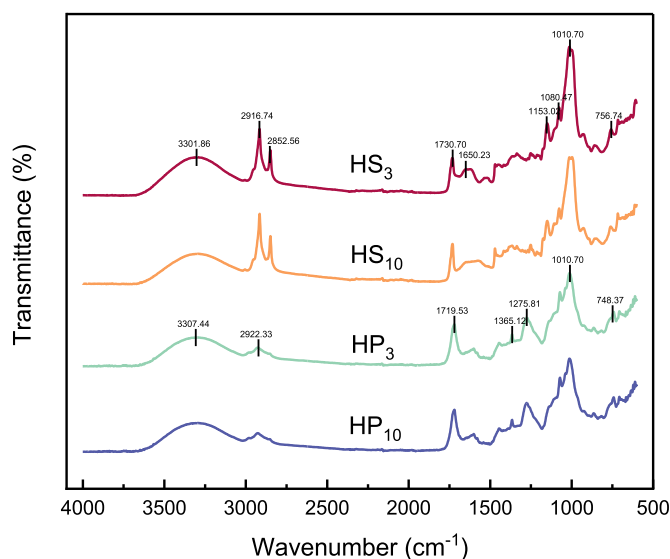


Fig. 1. FTIR spectra of the hydrocolloids obtained from the peel (HP₃; HP₁₀) and the seed (HS₃; HS₁₀) of the mango Tommy fruit.

the C–O and C–C bonds, as well as the glycosidic bonds (C–O–C) and C–O–H bonds (Bostan et al., 2010; Pourfarzad et al., 2021). The multiple peaks observed between 1100 and 1400 cm⁻¹ are indicative of a typical polysaccharide profile commonly found in hydrocolloids (Pal et al., 2005). These characteristic peaks are associated with various vibration modes of the molecular structure of polysaccharides (Hong et al., 2021), which are detected more clearly in HP samples; this profile is similar to other hydrocolloids extracted from plant materials, such as guar gum, a galactomannan from the legume *Cyanopsis teragonolobus*, and is also comparable to the high molecular weight fraction of pectin fruit jelly, with bands between 1374 and 1274 attributed to vibrations of carboxyl groups capable of forming strong gels (Čopíková et al., 2001). The bands between 1650 cm⁻¹ are related to the functional groups of amide I and amide II, respectively, which are associated with the presence of proteins that are more representative in samples HS₃ and HS₁₀ (Mata-Miranda et al., 2017). In general, hydrocolloid systems were obtained in all solubilizations performed according to the proposed methodology, showing the effect of pH and temperature as the experimental variables. It was observed that, at a temperature of 80°C, pH 3 and pH 10, the highest yields were observed, which were also evaluated in a previous study (Marsiglia-Fuentes et al., 2022). The hydrocolloids obtained from the seeds, in terms of extraction conditions, are rich in proteins and fats, and considering this functional characteristic, they proved to be more suitable for forming strong gels, whereas the hydrocolloids from the peel, rich in carbohydrates, proved to be more suitable for emulsifying applications. However, the extraction pH does not significantly affect the composition, although hydrocolloids extracted under acidic conditions had slightly lower extraction yields and stabilized the o/w emulsions much better, especially. Taking into account all factors, the hydrocolloid extracted from the mango peel at pH 3 has the most favorable functional properties for aqueous gel systems and stabilizing oil-in-water emulsions.

3.2. Hydrodynamic analysis and molecular weight

Specific viscosity provides the contribution of the polymer to the viscosity of a polymeric solution relative to the viscosity of the pure solvent. This parameter provides valuable information on the behavior of a polymer in solution and its interaction with the solvent (Karakus et al., 2020). Table 4 shows the relative viscosity and specific viscosity data for water solutions of different extracts of mango peel and seeds, at a concentration of 0.5 % v / v, and other viscometric parameters that

Table 3

pH and proximal composition of hydrocolloids extracted from mango peel and seeds.

Parameter	HP ₃	HP ₁₀	HS ₃	HS ₁₀
TTA (mg of citric acid /100 mL)	0.43 ± 0.99 ^a	0.06 ± 0.09 ^b	0.44 ± 0.63 ^a	0.08 ± 0.43 ^b
pH	4.35 ± 0.75 ^b	8.25 ± 0.32 ^a	4.56 ± 0.19 ^b	8.16 ± 0.78 ^a
Moisture (%)	13.11 ± 0.78 ^a	11.14 ± 0.66 ^a	12.16 ± 0.85 ^a	12.97 ± 0.24 ^a
Protein (%)	0.38 ± 0.03 ^b	0.35 ± 0.03 ^b	33.42 ± 0.03 ^a	32.45 ± 0.03 ^a
Ash (%)	8.50 ± 0.31 ^b	9.15 ± 0.44 ^a	7.30 ± 0.75 ^c	7.82 ± 0.34 ^c
Fat (%)	2.86 ± 0.23 ^a	2.75 ± 0.11 ^a	16.85 ± 0.12 ^b	17.33 ± 0.26 ^b
Carbohydrate (%)	75.15 ± 0.20 ^a	76.61 ± 0.53 ^a	29.85 ± 1.31 ^b	29.43 ± 0.38 ^b

The results are presented as mean ± standard deviation. Different letters within each row indicate significant differences ($p < 0.05$).

Table 4

Hydrocolloids viscosimetry extracted from the peel (HP₃; HP₁₀) and seed (HS₃; HS₁₀) of mango tomy (*Mangifera indica*).

Viscosity type	HP ₃	HP ₁₀	HS ₃	HS ₁₀
Relative viscosity (η_{rel})	1.04 ±0.02 ^a	1.04±0.06 ^a	1.03±0.03 ^a	1.03±0.03 ^a
Specific viscosity (η_{sp})	0.04 ±0.01 ^b	0.04±0.01 ^b	0.03±0.01 ^a	0.03±0.01 ^a
Reduced viscosity (η_{red})	0.09 ±0.05 ^b	0.08±0.03 ^b	0.05±0.01 ^a	0.05±0.02 ^a
Intrinsic viscosity ($[\eta]$, dL/g)	1.96 ±0.02 ^a	1.96±0.03 ^a	1.97 ±0.06 ^{ab}	1.98±0.06 ^b
Molecular Weigh (M_v), g/mol)	101,515 ±850 ^a	101,516 ±220 ^a	102,936 ±150 ^b	103,122 ±460 ^b

The results are presented as mean ± standard deviation. Different letters within each row indicate significant differences ($p < 0.05$).

can be determined from these, i.e., the reduced and intrinsic viscosities. The intrinsic viscosity of each hydrocolloid was determined from the Solomon-Ciuta equation, while the average molecular weight of viscosity was estimated from the Mark-Houwink-Sakurada equation (MHS) (Eq. 5). From these results, it is observed that the samples extracted from the peel and seeds at different pHs produced very similar intrinsic viscosity values that do not vary significantly, with identical values (1.96 dL/g) for the HP₃ and HP₁₀ samples, and 1.97 and 1.98 dL/g for the HS₃ and HS₁₀ samples, respectively, at 25 °C. These results are lower than those reported for xanthan gum (49.2 dL/g) (Brunchi et al., 2014), basil seed gum (39.17 dL/g) (Naji-Tabasi and Razavi, 2016), tara gum (11.07 dL/g) (Huamaní-Meléndez et al., 2021) or tamarind seed gum (4.7 dL/g) (Khouvilay and Sittikijyothin, 2012), higher than the values obtained from *Lepidium sativum* seed gum (0.726 dL/g) (Razmkhah

et al., 2016), and very similar to those obtained by Fathi et al., (2018a) for polysaccharides extracted from *Lallemantia ibrica* seeds (1.96 dL/g at 25 °C). The molecular characteristics of natural polymers have a crucial impact on their bioactivity and functional qualities. Thus, polysaccharides with a high molecular weight have a low tendency to be adsorbed at the air-water interface, but their thickening and gelling capabilities can greatly improve the stability of food matrices (Martinez et al., 2005). The viscosity-average molecular weight (M_v) of the hydrocolloids estimated from the intrinsic viscosity data gave values for the hydrocolloids extracted from the peel (HP₃ and HP₁₀) and seeds (HS₃ and HS₁₀) of 101,515 and 102,580 g/mol, respectively. Hydrocolloids obtained from the seeds have a slightly higher molecular weight. Likewise, these results are similar to the molecular weights found for guar gum (112,000 g/mol) (Khouryieh et al., 2007). In principle, high-molecular-weight hydrocolloids provide enhanced gelling capacity and ability for structuring of colloidal systems (Faria et al., 2011). Utilizing waste materials such as mango peel and seeds for the extraction of hydrocolloids presents a significant opportunity to enhance sustainability and resource efficiency in the food industry.

3.3. SEM analysis of hydrocolloids

SEM was carried out to see if the alkaline and acidic extraction conditions could affect the structure of the peel and seed hydrocolloids, showing some porosity that was more evident in the peel samples when extracted under acidic conditions. SEM micrographs of hydrocolloids derived from mango peel and seeds are shown in Fig. 2. The HP₃ (C) and HS₃ (A) samples have a less compact structure than the HP₁₀ (D) and HS₁₀ (B) samples. Based on the extraction conditions, it can be concluded that at acidic pH (A and C) the formation of cavities on the

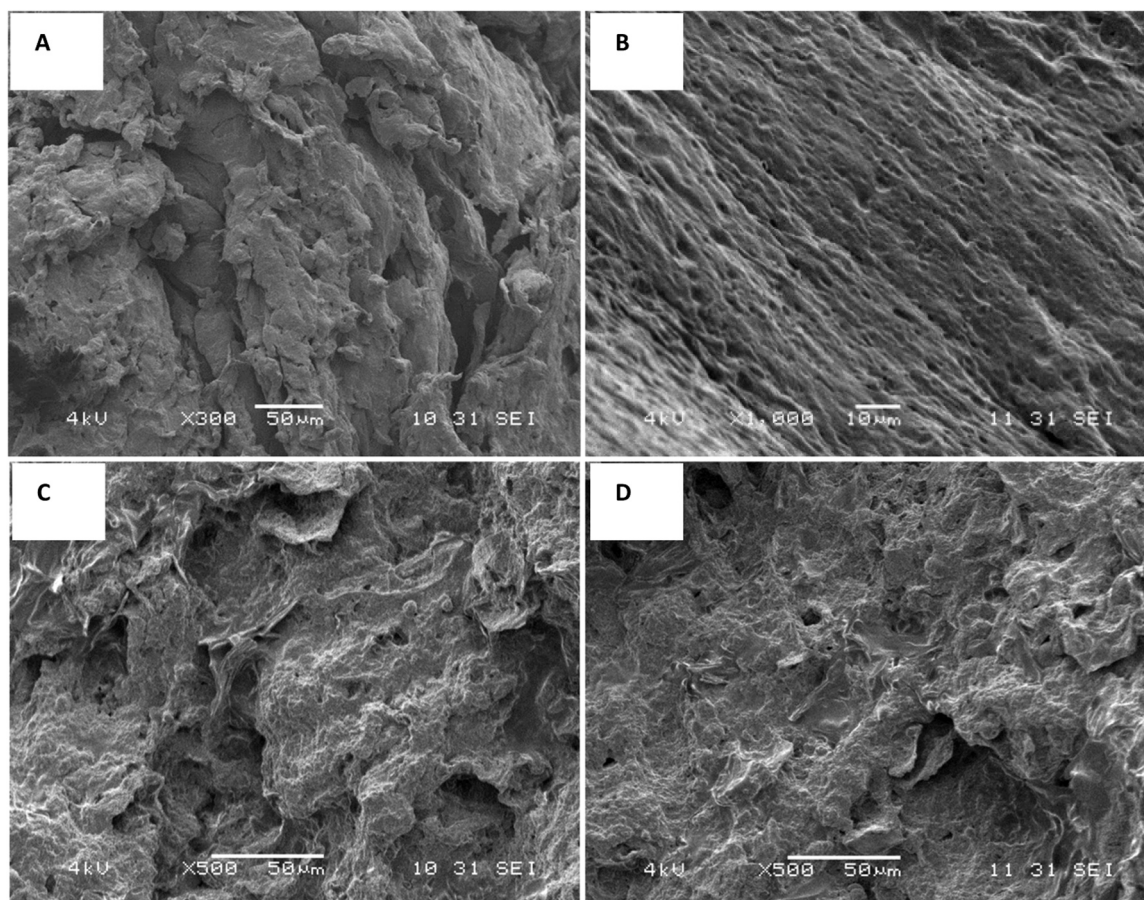


Fig. 2. SEM micrographs of hydrocolloids extracted from mango seeds [HS₃ (A); HS₁₀ (B)] and peel [HP₃ (C); HP₁₀ (D)].

surface of the hydrocolloids is favored for both samples compared to samples extracted at basic pH (B and D). These variations in microstructure may influence the quality, volume, stiffness and texture profile of derived food products (Manohar and Rao, 1999). An acid pH can cause the breakage of polymer chains during the extraction of hydrocolloids, which makes the material to be more heterogeneous. This fact may enhance the ability to increase the viscosity of hydrocolloidal systems, such as hydrogels, resulting in better interactions with water and minimizing the time and ability of the material to gel when subjected to moderate heating (Larrosa, 2014). On the other hand, sample HS₁₀ (B) has a smooth surface and compact structure, which can be influenced by fat content, leading to the generation of more homogeneous regions, indicating that the matrix of these samples can be protected from hydration (Reaz et al., 2023).

3.4. Rheological behavior

3.4.1. Steady-state viscous flow

From a sensory point of view, examining the flow behavior of polymeric systems at low shear rates provides valuable insight into characterizing the mouthfeel and consistency of food during oral consumption (Morris, 1990). Understanding how food responds to gentle forces, such as those encountered during chewing and swallowing, is essential to assess the sensory attributes and overall texture of food products. On the contrary, having a precise understanding of the viscosity/strain rate relationship at high shear rates is essential to investigate the flow behavior of gum solutions during various operations, such as spray drying and fluid pumping. These processes involve high shear forces, and knowing how the viscosity of gum solutions changes under such conditions is essential to efficiently optimize and control these industrial operations (Fathi et al., 2018b). Fig. 3 shows the viscosity versus shear rate plots for the hydrocolloid formulations HS₃ (seed) and HP₃ (peel) at different concentrations (1, 2.5 and 5 %) compared to the viscosity of guar gum at 1 % taken as a reference. In the shear rate range studied (0.01–1000 s⁻¹), an apparent shear thinning response was found in all cases. As is well known, as the shear rate increases, the macromolecular chains of the biopolymer align in the direction of flow, the entanglement among polymer chains decreases, and therefore the viscosity decreases (Koocheki et al., 2013). This study has highlighted the expected shear thinning properties. At certain concentrations, hydrocolloids should confer pseudoplastic properties to the

gels. From this perspective, the comparison of viscosity changes with the shear rate in relation to the inherent viscosity of polymers is directly related to the quality of the solvent, the macromolecular structure, and the molecular weight (Cerqueira et al., 2009). When the viscous flow curves are analyzed, it becomes evident that the hydrocolloid formulations derived from the seeds exhibited a viscosity higher than that of the formulations derived from the peel, especially at low shear rates, which is related to the slightly higher molecular weight.

The experimental data of the flow curves were adjusted to the Williamson model:

$$\eta = \frac{\eta_0}{1 + (k\dot{\gamma})^n} \quad (6)$$

where $\dot{\gamma}$ is the shear rate, k is the consistency index, and n is the rate index, and η_0 is the zero-rate viscosity. The values of these fitting parameters are presented in Table 5. The minimum value of the coefficient of determination ($R^2 > 0.996$) indicates an excellent fit to the experimental data. In all cases, the value of $n < 1$ confirmed the shear-thinning behavior of the hydrocolloids. As the concentration of hydrocolloids in the solution increased, the viscosity values of the resulting hydrogels

Table 5

Williamson model rheological parameters for gels formulated with hydrocolloids extracted from peel (HP₃) and seed (HS₃) of mango Tommy fruit.

Hydrocolloidal system	% Hydrocolloids	η_0	k	n	R^2
HP ₃ -1	1	0.54 ± 0.01 ^a	0.31 ± 0.01 ^{ab}	0.66 ± 0.03 ^a	0.998
HP ₃ -2.5	2.5	0.86 ± 0.04 ^b	0.51 ± 0.01 ^c	0.73 ± 0.01 ^b	0.997
HP ₃ -5	5	2.64 ± 0.01 ^d	0.41 ± 0.02 ^b	0.67 ± 0.03 ^a	0.999
HS ₃ -1	1	1.03 ± 0.02 ^b	0.21 ± 0.06 ^a	0.73 ± 0.02 ^b	0.996
HS ₃ -2.5	2.5	1.89 ± 0.03 ^c	0.24 ± 0.01 ^a	0.68 ± 0.05 ^a	0.999
HS ₃ -5	5	5.94 ± 0.03 ^e	0.47 ± 0.04 ^b	0.72 ± 0.01 ^b	0.998
Guar gum (1 %)	1	0.49 ± 0.02 ^a	0.22 ± 0.01 ^a	0.63 ± 0.02 ^a	0.998

Results are expressed as mean ± standard deviation. Different letters within each column mean significant differences ($p < 0.05$).

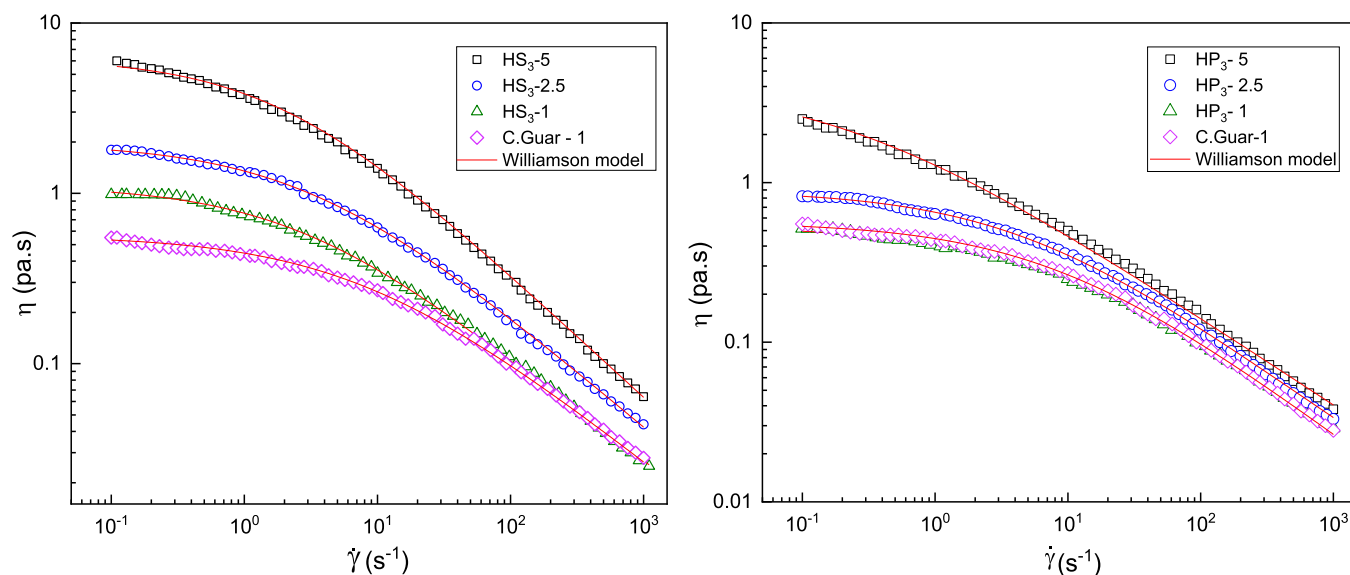


Fig. 3. Viscous flow curves and fitting to the Williamson model for hydrogels derived from hydrocolloids extracted from the seed (HS₃) and peel (HP₃) of mango Tommy fruit at different concentrations (1, 2.5, 5 %). Guar gum-derived hydrogel at 1 % is included as a control system.

showed a relative increase. Furthermore, as mentioned above, hydrocolloid formulations obtained from mango seeds showed a higher viscosity than those found in hydrocolloids obtained from the peel. For instance, the low-shear rate limiting viscosity of HS₃-5 sample was 5.04 ± 0.03 Pa.s, while the counterpart of the peel-extracted hydrocolloid (HP₃-5) was 2.64 ± 0.01 Pa.s. These higher values generally found in hydrogels obtained from mango seed hydrocolloids must be attributed to both the slightly higher viscosity-average molecular weight (see Table 3) and the different composition, which in turn influence the gelatinization process. Such insights are valuable in understanding the behavior and potential applications of these hydrocolloids in various industrial settings (Lastra-Ripoll et al., 2022a). On the other hand, the viscosity vs. shear rate plot for the guar gum sample taken as a reference, prepared at a concentration of 1 % by weight, was almost consistent with the HP₃-1 viscous flow curve, while the HS₃-1 sample, at the same concentration of 1 % by weight, provided a higher viscosity than the control.

3.4.2. Curing

Aiming to study the heat-induced gelling process (sol-gel), the impact of a heat treatment on the rheological properties of mango peel and seeds-derived hydrocolloid formulations was analyzed by applying ascending/descending temperature ramps, reaching a maximum temperature of 70 °C, and the variation of the storage modulus, G' , was monitored. The upward temperature ramp was applied at 4°C/min, then the temperature was maintained constant at 70 °C for 20 min, and then a downward temperature ramp at 4°C/min was applied to cool the sample down to 25 °C. Fig. 4 illustrates the evolution of G' over time for the different gel-forming solutions (at 1 %, 2.5 %, 5 % concentrations). The curing behavior observed in all samples is qualitatively similar. In the second region, where the temperature remains constant at 70 °C (cycle B), G' exhibits a rapid increase, which is followed by stabilization by cooling the sample (cycle C). Furthermore, while at 2.5 and 5 % wt concentrations G' increased to comparable values, below 2.5 % wt, that is, 1 % wt, the enhancement of gel strength was noticeably inferior. In this case, the control of the guar gum sample (at 1 % wt.) behaves against thermal treatments similarly to the hydrocolloid formulations derived from mango seeds and peels at 2.5 and 5 % by weight. These results shed light on the temperature-dependent gelation behavior of these hydrocolloid solutions and their potential implications in the food industry. The observed evolution of the storage modulus is attributed to the unique properties of hydrocolloids in response to heat. During the heating process, the hydrocolloids expand, exposing functional groups capable of forming gel networks. This expansion contributes to the

initial increase in G' values as the gel structure begins to develop and, when the solution is cooled, the three-dimensional gel network becomes more stabilized, resulting in further hardening of the matrix and eventually an additional slight increase in the G' values. In this case, during the downward ramp (cycle C), the cooling rate does not seem to greatly influence the final value of the linear viscoelastic functions, and the G' values remain almost constant or slightly increase, indicating a favorable behaviour in the gel-strengthening process. The final G' values are generally higher in HP hydrocolloids-derived gels than in those obtained from HS samples, probably due to the higher carbohydrate content, despite the lower viscosity achieved under shear conditions (see Fig. 3). Understanding the gelation process and its effect on the rheological properties of hydrocolloids provides valuable insight into optimizing their applications in different formulations and processing techniques (Gurram and Author, 2022; Pirsá and Hafezi, 2023). It is essential to consider the time-temperature history of hydrocolloid solutions to optimize their applications in various processes, as their gelling behavior can be influenced by such factors. Understanding the conditions that favour or hinder gel formation and gel strength allows for better control and use of hydrocolloids in various industrial and food applications (Chen and Dickinson, 1998).

3.4.3. Linear viscoelasticity

Stress sweep tests were conducted at 25 °C to identify the viscoelastic linear region of the hydrocolloid formulations before and after applying the heat treatment previously discussed in the curing tests. The samples showed a linear viscoelastic region within the range of 1.0–20.0 Pa. In this range, frequency sweeps were performed afterwards. Fig. 5 shows the mechanical spectra of gels derived from samples HP₃ and HS₃ at various concentrations (1–5 %) obtained at 25 °C. In all cases, both the storage (G') and loss (G'') moduli slightly increased with frequency and the values of G' were consistently higher than those of G'' , suggesting a predominantly elastic behavior without a crossover point in the frequency range studied, whereas G'' exhibited a soft minimum at medium or low frequencies. This evolution of SAOS moduli corresponds to the "plateau" region of the mechanical spectrum, which is characteristic of weak gels. However, some differences in the extent of the "plateau" region were observed in the frequency range studied, depending on the type and concentration of the hydrocolloid incorporated. Higher percentages of hydrocolloids (5 %) resulted in a more structured gel with increased strength, which is attributed to the enhanced entanglement network and aggregation of the biopolymer chains. These observations offer valuable information on the rheological behavior and mechanical properties of mango peel- and seeds-derived hydrocolloid gels, providing essential information to optimize their applications in food

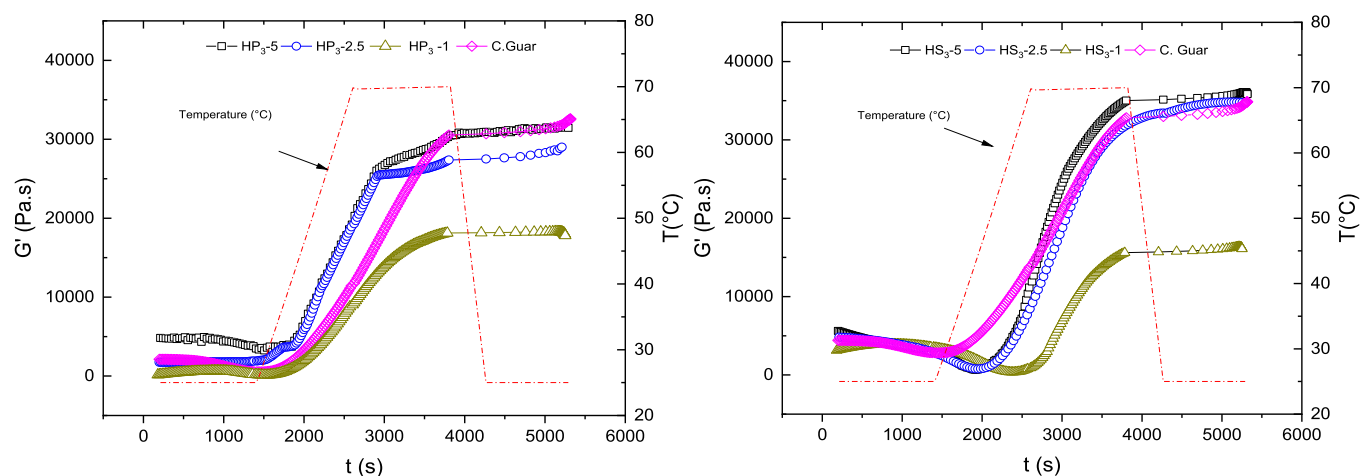


Fig. 4. Evolution of the storage modulus over time during the application of temperature ramps, for hydrogels derived from hydrocolloids extracted from the seed (HS₃) and peel (HP₃) of mango Tommy fruit, containing 1, 2.5 and 5 % w/w hydrocolloids. Guar gum-derived hydrogel at 1 % is included as a control system.

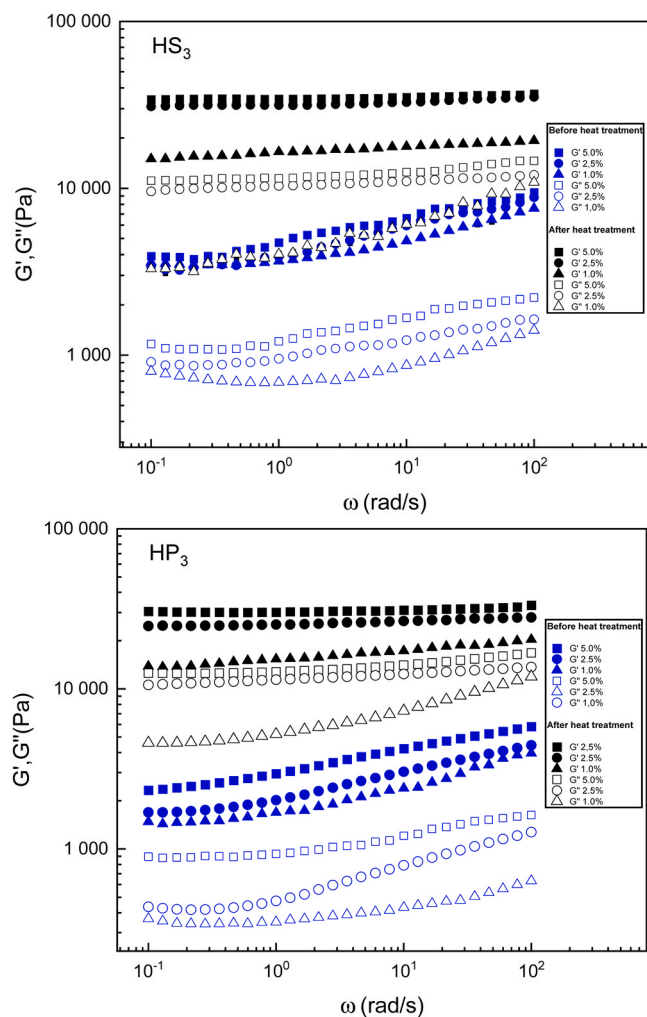


Fig. 5. Mechanical spectra of hydrogels derived from hydrocolloids extracted from the seed (HS₃) and the peel (HP₃) of mango Tommy fruit, containing 1, 2.5 and 5% w/w hydrocolloids, obtained after applying the heat treatment shown in Fig. 4. For the sake of comparison, the mechanical spectra of dispersions before heating are also shown.

and industrial formulations (Arab et al., 2023). The findings indicated that even solutions at low concentrations (1 %) showed elastic behavior at low frequencies. This behavior can be attributed to the large molecular weight and the high degree of branching in hydrocolloid molecules, which contribute to their elastic nature (Wang et al., 2019). For similar concentrations of hydrocolloids, this behavior has been observed in other hydrocolloids, such as the *Alyssum homolocarpum* seed hydrocolloid (Anvari et al., 2016), *Lepidium perfoliatum* seed hydrocolloid (Hesarinejad et al., 2014), basil seed gum (Rafe and Razavi, 2013) or quince seed gum (Wang et al., 2019). The achievement of relatively elastic formulations with low concentrations underscores the unique rheological characteristics of these hydrocolloids that make them suitable for various applications in the food and industrial sectors. Moreover, mango seed-derived hydrocolloids provide gels with G' values higher than those obtained from HP samples regardless of the hydrocolloid concentration, again probably because of the higher protein content. For example, the HS₃-5 sample reaches G' values of around 35,000 Pa, compared to those obtained with HP₃-5 with values of approximately 30,000 Pa. Understanding these properties is crucial for formulating stable and functional products, as well as for tailoring their performance in specific applications.

Finally, Fig. 5 also shows the comparison of the mechanical spectra of the gels obtained before and after applying the thermal curing

treatment. As can be seen, a significant increase in the values of both SAOS functions is apparent compared to those of the initial state of the gels before they are subjected to any thermal treatment. This indicates that when the hydrocolloid formulations were heated and then cooled, the three-dimensional structure of the gel is strengthened, resulting in a significantly increased stiffness.

3.5. Emulsion stabilizing properties

In Fig. 6, the droplet size distributions (DSD) of emulsions prepared with aqueous solutions containing samples HP₃, HP₁₀, HS₃ and HS₁₀, at a concentration of 1.2 %, are shown as a function of ageing. On day 1, the emulsions exhibit a relatively wide size distribution that varies approximately from 0.5 to 200 μm . On day 4, a slight increase in particle size was observed for HS₃ and HS₁₀ emulsions, while emulsions HP₃ and HP₁₀ remained relatively stable. On day 6, the polymodal distribution is still maintained, but a separation phase is clearly detected in the upper part of the HS₃ and HS₁₀ samples, evincing creaming, and an incipient separation was also observed for the HP₁₀ sample in the lower part. After 8 days, the HP₁₀, HS₃, and HS₁₀ emulsions separate, while the HP₃ sample experiences minimal separation. These results clearly indicate a close relationship between droplet size and emulsion stability. Emulsions with smaller droplet sizes tend to remain stable for a longer period.

Table 6 provides more detailed information regarding DSD, presenting the values of D_{10} , D_{50} , and D_{90} , which correspond to the particle size in which 10 %, 50 % and 90 % of the cumulative distribution are included. The mean values of D_{10} , D_{50} , and D_{90} ranged between 1.65 and 19.40 μm , 10.04–82.52 μm , and 30.6–154.78 μm , respectively. These values also reflect the effect of storage time on the particle size distribution, with D_{10} showing the lowest degree of variability, followed by D_{50} , and D_{90} being the most representative or critical measure. The 10 % accumulated (D_{10}) corresponds to the smallest particles in the emulsion. As storage time progresses, the D_{10} values remain relatively stable, indicating minimal changes in the size of these colloidal fragments. However, the values of D_{50} may consider larger droplets and/or undissolved fragments of the hydrocolloids. Over time, the attractive forces between these particles cause them to increase in size and eventually coalesce into larger droplets, producing an increased D_{90} value. Analysis of D_{10} , D_{50} , and D_{90} provides valuable information on the dynamics of particle size distribution within the emulsions as they undergo storage. These findings contribute to the optimization of emulsion formulations and the control of their behavior in various applications. (Eraso-Grisales et al., 2022).

The zeta potential values (ζ) of the emulsions formulated with hydrocolloids derived from mango peel and seeds, as shown in Table 5, ranged from -17.63 to -11.12 mV. The decrease in ζ can be attributed to the limitation of the ionizable sites in the hydrocolloids polymer chains. The negative charge on these polymers is a critical parameter closely related to the physicochemical stability and composition of the emulsion. Firstly, it indicates the magnitude of repulsive or electrostatic forces between neighboring colloidal particles. A higher absolute value of the zeta potential, positive or negative, indicates stronger repulsive forces between particles, which can hinder aggregation and coalescence. In the context of emulsions, a higher negative zeta potential is generally desirable, as it contributes to greater stability by preventing droplet aggregation and creaming. Consequently, the lower (more negative) zeta potential of the HP₃ sample indicates stronger repulsive forces between colloidal particles, thus contributing to enhanced physical stability. Understanding the potential of zeta is crucial to designing emulsions with optimal stability and desired characteristics in industries such as food, cosmetics, and pharmaceuticals and helps to control the interactions between dispersed particles and fine-tune the formulation to meet specific requirements (Yu et al., 2016). The observed differences in the zeta potential and particle size among the samples studied emphasize the importance of the hydrocolloid structure and composition in stabilizing o/w emulsions.

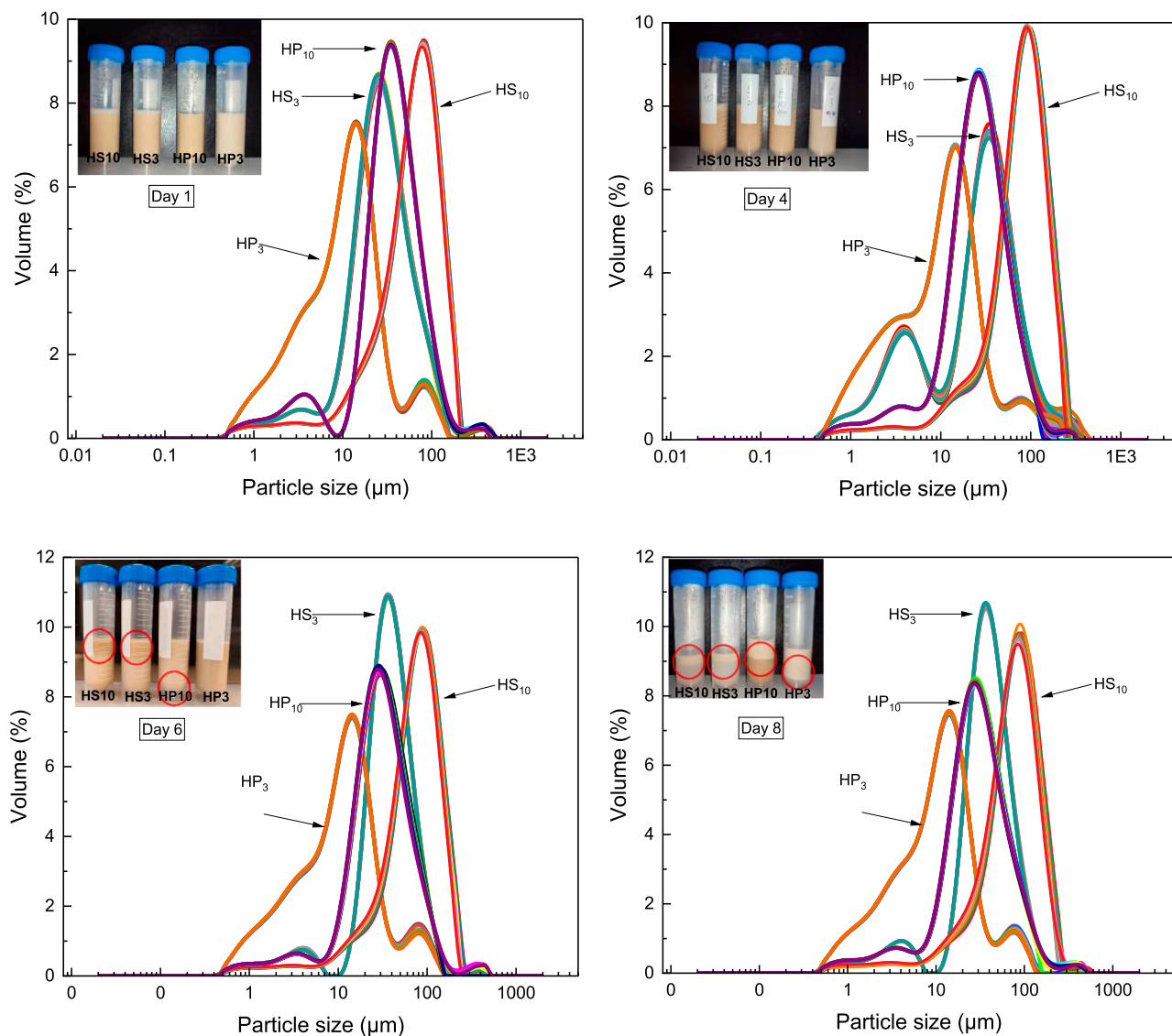


Fig. 6. Evolution of the droplet size distribution as a function of storage time (days) for emulsions prepared with hydrocolloids extracted from the peel (HP₃, HP₁₀) and the seed (HS₃; HS₁₀) of Tommy mango fruit.

4. Conclusions

Hydrocolloids extracted from Tommy mango presented in Peel (HP) are rich in carbohydrates, while seeds (HS) contain more proteins and fats, respectively. Morphological differences are evident, while HP exhibits a more irregular and porous structure compared to HS, especially notable at low pH levels. The average molecular weights HP and HS are approximately 101,515 g/mol and 102,580 g/mol. Both hydrocolloids can form hydrogels in water when heated at concentrations ranging from 1% to 5% by weight. These hydrogels exhibit shear-thinning behavior, conforming to the Williamson model. The gelation process can be monitored through curing tests, revealing lower critical temperatures for gelation in HS hydrocolloids compared to that of HP. The viscoelastic properties of the hydrogels increase with concentrations of 2.5% and 5%, providing comparable gel strengths. The emulsion derived from HS samples showed phase separation after 4 days, indicating instability, whereas the emulsion derived from HP₃ showed minimal separation even after 8 days. This difference in stability has been attributed to the significantly smaller mean droplet size and the more negative zeta potential achieved in the HP₃ sample-derived emulsion. In summary, the selection of Tommy mango residues, i.e.,

peel and seeds, and the extraction conditions greatly influence the composition and functional properties of derived hydrocolloids, which determines their preferential application. Hydrocolloids extracted from seeds, rich in proteins and fats, are more suitable to form stronger gels, while hydrocolloids from the peel, rich in carbohydrates, are more suitable for emulsifying applications. However, extraction pH does not significantly affect the composition, although hydrocolloids extracted under acidic conditions had slightly lower extraction yields and stabilized o/w emulsions much better, especially those obtained from the peel. Taken everything into consideration, the hydrocolloid extracted from the peel of mango, at pH 3, is the one with the optimal functional properties for both gelling aqueous systems and stabilizing o/w emulsions.

Funding

The Ministry of Science, Technology, and Innovation, MinCiencias - high-level human capital training program (Minciencias Bicentennial Doctoral Excellence Scholarships) with overall royalty system resources from the Colombian government (Bienio 2019–2020), managed through Colfuturo, funded this research. Thanks to the Research Vice-Rectorate

Table 6

Characteristic mean droplet size diameter and ζ potential values of emulsions prepared with hydrocolloids extracted from peel (HP₃, HP₁₀) and seed (HS₃; HS₁₀) of Tommy mango fruit.

Sample	Ageing (days)	ζ (mV)	D ₁₀ (μm)	D ₅₀ (μm)	D ₉₀ (μm)
HP ₃	1	-17.58 ^a	1.65±0.06 ^a	10.04 ±0.05 ^a	30.6±0.07 ^a
	4	-17.63 ^a	1.65±0.10 ^a	10.60 ±0.05 ^a	33.20±0.08 ^b
	6	-16.86 ^{ab}	1.92±0.01 ^a	11.21 ±0.10 ^a	33.40±0.74 ^b
	8	-16.47 ^b	1.93±0.02 ^a	11.80 ±0.07 ^a	33.70±0.11 ^b
HP ₁₀	1	-16.38 ^b	19.31 ±0.04 ^{ef}	76.20 ±0.37 ^e	148.87 ±0.25 ^h
	4	-15.43 ^c	19.40 ±0.34 ^e	78.20 ±0.37 ^e	149.36 ±0.72 ^h
	6	-15.45 ^c	17.70 ±0.18 ^e	80.40 ±0.27 ^f	154.02 ±0.21 ⁱ
	8	-14.56 ^c	15.80 ±0.14 ^d	82.52 ±0.33 ^f	154.78 ±0.70 ^j
HS ₃	1	-12.05 ^d	16.21 ±0.21 ^{de}	36.55 ±0.07 ^d	78.54 ±0.01 ^f
	4	-12.13 ^d	15.76 ±0.03 ^d	37.02 ±0.21 ^d	81.62 ±0.27 ^g
	6	-12.05 ^d	14.60 ±0.07 ^d	37.21 ±0.16 ^d	81.10 ±0.05 ^g
	8	-11.12 ^{de}	12.61 ±0.71 ^c	37.52 ±0.19 ^d	82.31 ±0.09 ^g
HS ₁₀	1	-12.75 ^d	18.32 ±0.01 ^e	24.16 ±0.21 ^b	60.14±0.08 ^c
	4	-11.45 ^e	12.75 ±0.05 ^c	25.7±0.18 ^b	63.20±0.01 ^d
	6	-11.70 ^e	10.65 ±0.18 ^b	29.8±0.06 ^c	75.81±0.28 ^e
	8	-11.47 ^e	9.93±0.09 ^b	28.41 ±0.03 ^c	77.33 ±0.02 ^{ef}

Results are expressed as mean ± standard deviation. The different letters within each column are significantly different ($p < 0.05$).

of the University of Cartagena for strengthening plans to obtain research for research groups classified by (MINCIENCIAS) that support the main-line research of a doctorate in the University of Cartagena, year of 2022, according to Resolution No. 00475 of 2022 and Start Act 002–2022, which allowed the funding for the presentation of this research.

CRediT authorship contribution statement

José M. Franco: Writing – review & editing, Methodology, Formal analysis, Conceptualization. **Ronald Marsiglia-Fuentes:** Writing – review & editing, Resources, Investigation. **Luis Alberto Garcia Zapateiro:** Writing – original draft, Resources, Project administration, Conceptualization.

Declaration of Competing Interest

The authors whose names are listed below certify that:

All authors have participated in (a) conception and design, or analysis and interpretation of the data; (b) drafting the article or revising it critically for important intellectual content; and (c) approval of the final version. This manuscript has not been submitted to, nor is under review at, another journal or other publishing venue.

The authors have no affiliation with any organization with a direct or indirect financial interest in the subject matter discussed in the manuscript.

References

- Anvari, M., Tabarsa, M., Cao, R., You, S., Joyner Melito, H.S., Behnam, S., Rezaei, M., 2016. Compositional characterization and rheological properties of an anionic gum from *Alyssum homolocarpum* seeds. *Food Hydrocoll.* 52, 766–773. <https://doi.org/10.1016/j.foodhyd.2015.07.030>.
- Arab, K., Ghanbarzadeh, B., Karimi, S., Ebrahimi, B., Hosseini, M., 2023. Gelling and rheological properties of a polysaccharide extracted from *Ocimum album* L. seed. *Int. J. Biol. Macromol.* 246, 125603 <https://doi.org/10.1016/j.ijbiomac.2023.125603>.
- Beer, M.U., Wood, P.J., Weisz, J., 1999. A simple and rapid method for evaluation of Mark–Houwink–Sakurada constants of linear random coil polysaccharides using molecular weight and intrinsic viscosity determined by high performance size exclusion chromatography: application to guar galactomannan. *Carbohydr. Polym.* 39 (4), 377–380. [https://doi.org/10.1016/S0144-8617\(99\)00017-X](https://doi.org/10.1016/S0144-8617(99)00017-X).
- Bhusari, S.N., Muzaffar, K., Kumar, P., 2014. Effect of carrier agents on physical and microstructural properties of spray dried tamarind pulp powder. *Powder Technol.* 266, 354–364. <https://doi.org/10.1016/j.powtec.2014.06.038>.
- Blok, A.E., Bolhuis, D.P., Arnaudov, L.N., Velikov, K.P., Stieger, M., 2023. Influence of thickeners (microfibrillated cellulose, starch, xanthan gum) on rheological, tribological and sensory properties of low-fat mayonnaises. *Food Hydrocoll.* 136, 108242 <https://doi.org/10.1016/j.foodhyd.2022.108242>.
- Borah, D., Rethinam, G., Gopalakrishnan, S., Rout, J., Alharbi, N.S., Alharbi, S.A., Nooruddin, T., 2020b. Ozone enhanced production of potentially useful exopolymers from the cyanobacterium *Nostoc muscorum*. *Polym. Test.* 84, 106385 <https://doi.org/10.1016/j.polymertesting.2020.106385>.
- Borah, D., Rethinam, G., Gopalakrishnan, S., Rout, J., Alharbi, N.S., Alharbi, S.A., Nooruddin, T., 2020a. Ozone enhanced production of potentially useful exopolymers from the cyanobacterium *Nostoc muscorum*. *Polym. Test.* 84, 106385 <https://doi.org/10.1016/j.polymertesting.2020.106385>.
- Bostan, A., Razzavi, S.M.A., Farhoosh, R., 2010. Optimization of hydrocolloid extraction from wild sage seed (*Salvia macrosiphon*) using response surface. *Int. J. Food Prop.* 13 (6), 1380–1392. <https://doi.org/10.1080/10942910903079242>.
- Brunchi, C.E., Morariu, S., Bercea, M., 2014. Intrinsic viscosity and conformational parameters of xanthan in aqueous solutions: salt addition effect. *Colloids Surf. B: Biointerfaces* 122, 512–519. <https://doi.org/10.1016/j.colsurfb.2014.07.023>.
- Cao, J., Tong, X., Cheng, J., Peng, Z., Yang, S., Cao, X., Wang, M., Wu, H., Wang, H., Jiang, L., 2023. Impact of pH on the interaction between soy whey protein and gum arabic at oil–water interface: structural, emulsifying, and rheological properties. *Food Hydrocoll.* 139, 108584 <https://doi.org/10.1016/j.foodhyd.2023.108584>.
- Cerqueira, M.A., Pinheiro, A.C., Souza, B.W.S., Lima, Á.M.P., Ribeiro, C., Miranda, C., Teixeira, J.A., Moreira, R.A., Coimbra, M.A., Gonçalves, M.P., Vicente, A.A., 2009. Extraction, purification and characterization of galactomannans from non-traditional sources. *Carbohydr. Polym.* 75 (3), 408–414. <https://doi.org/10.1016/j.carbpol.2008.07.036>.
- Chen, J., Dickinson, E., 1998. Viscoelastic properties of heat-set whey protein emulsion gels. *J. Texture Stud.* 29 (3), 285–304. <https://doi.org/10.1111/j.1745-4603.1998.tb00171.x>.
- Chignola, R., Mainente, F., Zoccatelli, G., 2022. Rheology of individual chitosan and polyphenol/chitosan microparticles for food engineering. *Food Hydrocoll.* 132, 107869 <https://doi.org/10.1016/j.foodhyd.2022.107869>.
- Čopíková, J., Černá, M., Novotná, M., Kaasová, J., Synytsya, A., 2001. Application of FT-IR spectroscopy in detection of food hydrocolloids in confectionery jellies and food supplements. *Czech J. Food Sci.* 19 (2), 51–56. <https://doi.org/10.17221/6575-CJFS>.
- Cortez-Trejo, M.C., Loarca-Piña, G., Figueroa-Cárdenas, J.D., Manríquez, J., Mendoza, S., 2022. Gel properties of acid-induced gels obtained at room temperature and based on common bean proteins and xanthan gum. *Food Hydrocoll.* 132, 107873 <https://doi.org/10.1016/j.foodhyd.2022.107873>.
- da Costa, M.P.M., Delpech, M.C., de Mello Ferreira, I.L., de Macedo Cruz, M.T., Castanharo, J.A., Cruz, M.D., 2017. Evaluation of single-point equations to determine intrinsic viscosity of sodium alginate and chitosan with high deacetylation degree. *Polym. Test.* 63, 427–433. <https://doi.org/10.1016/j.polymertesting.2017.09.003>.
- De, A., Malpani, D., Das, B., Mitra, D., Samanta, A., 2020. Characterization of an arabinogalactan isolated from gum exudate of *Odina wodioides* Roxb.: Rheology, AFM, Raman and CD spectroscopy. *Carbohydr. Polym.* 250 <https://doi.org/10.1016/j.carbpol.2020.116950>.
- Dickinson, E., 2003. Hydrocolloids at interfaces and the influence on the properties of dispersed systems. *Food Hydrocoll.* 17 (1), 25–39. [https://doi.org/10.1016/S0268-005X\(01\)00120-5](https://doi.org/10.1016/S0268-005X(01)00120-5).
- Eitex, T.T., 2017. Valorisation of Mango Fruit By-products: Physicochemical Characterisation and Future Prospect (Vol. 50). Online. www.iiste.org.
- Eraso-Grisales, S., Cortes-Rodríguez, M., Castaño-Peláez, H.I., Hurtado-Benavides, A., 2022. Enzymatic hydrolysis of a colloidal system based on cape gooseberry. *Food Sci. Technol. (Braz.)* 42. <https://doi.org/10.1590/FST.67820>.
- Farahmandfar, R., Naji-Tabasi, S., 2020. Influence of different salts on rheological and functional properties of basil (*Ocimum basilicum* L.) seed gum. *Int. J. Biol. Macromol.* 149, 101–107. <https://doi.org/10.1016/j.ijbiomac.2020.01.170>.
- Faria, S., De Oliveira Petkowicz, C.L., De Moraes, S.A.L., Terrones, M.G.H., De Resende, M.M., De Frana, F.P., Cardoso, V.L., 2011. Characterization of xanthan gum produced from sugar cane broth. *Carbohydr. Polym.* 86 (2), 469–476. <https://doi.org/10.1016/j.carbpol.2011.04.063>.
- Fathi, M., Emam-Djomeh, Z., Sadeghi-Varkani, A., 2018a. Extraction, characterization and rheological study of the purified polysaccharide from *Lallemantia ibrica* seeds.

- Int. J. Biol. Macromol. 120, 1265–1274. <https://doi.org/10.1016/J.IJBIOMAC.2018.08.159>.
- Fathi, M., Emam-Djomeh, Z., Sadeghi-Varkani, A., 2018b. Extraction, characterization and rheological study of the purified polysaccharide from *Lallelantia ibrica* seeds. Int. J. Biol. Macromol. 120, 1265–1274. <https://doi.org/10.1016/J.IJBIOMAC.2018.08.159>.
- Gupta, S., Sharma, S., Kumar Nadda, A., Saad Bala Husain, M., Gupta, A., 2022. Biopolymers from waste biomass and its applications in the cosmetic industry: a review. Mater. Today: Proc. 68, 873–879. <https://doi.org/10.1016/J.MATPR.2022.06.422>.
- Gurram, S., Author, C., 2022. Role of hydrocolloids in food systems. Pharma Innov. J. 11 (8), 1748–1755. (www.thepharmajournal.com).
- Han, Z.T., Long, W.M., Zhang, T.H., Dong, Z.Y., Yan, J.X., 2022. Application of xanthan gum and konjac gum to improve the texture, rheological properties and microstructure of *Oviductus Ranae* gel. Int. J. Biol. Macromol. 222, 2709–2718. <https://doi.org/10.1016/J.IJBIOMAC.2022.10.052>.
- Hesarinejad, M.A., Koocheki, A., Razavi, S.M.A., 2014. Dynamic rheological properties of *Lepidium perfoliatum* seed gum: Effect of concentration, temperature and heating/cooling rate. Food Hydrocoll. 35, 583–589. <https://doi.org/10.1016/J.FOODHYD.2013.07.017>.
- Hong, T., Yin, J.Y., Nie, S.P., Xie, M.Y., 2021. Applications of infrared spectroscopy in polysaccharide structural analysis: progress, challenge and perspective. Food Chem.: X 12. <https://doi.org/10.1016/J.FOCHX.2021.100168>.
- Horwitz, W. (2010). Official methods of analysis of AOAC International. Volume I, agricultural chemicals, contaminants, drugs/edited by William Horwitz. (<https://repositorioinstitucional.ceu.es/handle/10637/3158>).
- Huamán-Meléndez, V.J., Mauro, M.A., Darras-Barbosa, R., 2021. Physicochemical and rheological properties of aqueous Tara gum solutions. Food Hydrocoll. 111, 106195. <https://doi.org/10.1016/J.FOODHYD.2020.106195>.
- Jones, K.L., Hu, B., Li, W., Fang, Y., Yang, J., 2022. Investigation of rheological behaviors of aqueous gum Arabic in the presence of crystalline nanocellulose. Carbohydr. Polym. Technol. Appl. 4, 100243. <https://doi.org/10.1016/J.CARPTA.2022.100243>.
- Karakus, S., Ilgar, M., Tan, E., Kahyaoglu, I.M., Tasaltin, N., Albayrak, I., Insel, M.A., Kilislioglu, A., 2020. Preparation and characterization of carboxymethyl cellulose/poly (ethylene glycol) -rosin pentaerythritolester polymeric nanoparticles: role of intrinsic viscosity and surface morphology. Surf. Interfaces 21, 100642. <https://doi.org/10.1016/J.SURFIN.2020.100642>.
- Kavya, M., Ranjit Jacob, A., Nisha, P., 2023. Pectin emulsions and emulgels: bridging the correlation between rheology and microstructure. Food Hydrocoll. 143, 108868. <https://doi.org/10.1016/J.FOODHYD.2023.108868>.
- Ke, Y., Dai, T., Xiao, M., Chen, M., Liang, R., Liu, W., Liu, C., Chen, J., Deng, L., 2022. Industry-scale microfluidizer system produced whole mango juice: effect on the physical properties, microstructure and pectin properties. Innov. Food Sci. Emerg. Technol. 75, 102887. <https://doi.org/10.1016/J.IFSET.2021.102887>.
- Khounvilay, K., Sittikijyothin, W., 2012. Rheological behaviour of tamarind seed gum in aqueous solutions. Food Hydrocoll. 26 (2), 334–338. <https://doi.org/10.1016/J.FOODHYD.2011.03.019>.
- Khouryieh, H.A., Herald, T.J., Aramouni, F., Alavi, S., 2007. Intrinsic viscosity and viscoelastic properties of xanthan/guar mixtures in dilute solutions: effect of salt concentration on the polymer interactions. Food Res. Int. 40 (7), 883–893. <https://doi.org/10.1016/j.foodres.2007.03.001>.
- Koocheki, A., Taherian, A.R., Bostan, A., 2013. Studies on the steady shear flow behavior and functional properties of *Lepidium perfoliatum* seed gum. Food Res. Int. 50 (1), 446–456. <https://doi.org/10.1016/J.FOODRES.2011.05.002>.
- Larrosa, V.J., 2014. Efectos de los hidrocoloides en las características fisicoquímicas y reológicas de pastas libres de gluten aptas para individuos celíacos. <https://doi.org/10.35537/10915/35442>.
- Lastra-Ripoll, S.E., Quintana, S.E., García-Zapateiro, L.A., 2022b. Chemical, technological, and rheological properties of hydrocolloids from sesame (*Sesamum indicum*) with potential food applications. Arab. J. Chem. 15 (10) <https://doi.org/10.1016/j.arabj.2022.104146>.
- Lastra-Ripoll, S.E., Quintana, S.E., García-Zapateiro, L.A., 2022a. Chemical, technological, and rheological properties of hydrocolloids from sesame (*Sesamum indicum*) with potential food applications. Arab. J. Chem. 15 (10) <https://doi.org/10.1016/J.ARABJC.2022.104146>.
- Liu, J., Shim, Y.Y., Tse, T.J., Wang, Y., Reaney, M.J.T., 2018b. Flaxseed gum a versatile natural hydrocolloid for food and non-food applications. Trends Food Sci. Technol. 75, 146–157. <https://doi.org/10.1016/J.TIFS.2018.01.011>.
- Liu, J., Shim, Y.Y., Tse, T.J., Wang, Y., Reaney, M.J.T., 2018a. Flaxseed gum a versatile natural hydrocolloid for food and non-food applications. Trends Food Sci. Technol. 75, 146–157. <https://doi.org/10.1016/J.TIFS.2018.01.011>.
- de Lourdes García-Magaña, M., García, H.S., Bello-Pérez, L.A., Sáyago-Ayerdi, S.G., de Oca, M.M.M., 2013. Functional properties and dietary fiber characterization of mango processing by-products (*Mangifera indica* L., cv Ataulfo and Tommy Atkins). Plant Foods Hum. Nutr. 68 (3), 254–258. <https://doi.org/10.1007/S11130-013-0364-Y>.
- Manohar, R.S., Rao, P.H., 1999. Effect of mixing method on the rheological characteristics of biscuit dough and the quality of biscuits. Eur. Food Res. Technol. 210 (1), 43–48. <https://doi.org/10.1007/S002170050530/METRICS>.
- Marçal, S., Pintado, M., 2021. Mango peels as food ingredient / additive: nutritional value, processing, safety and applications. Trends Food Sci. Technol. 114, 472–489. <https://doi.org/10.1016/J.TIFS.2021.06.012>.
- Marsiglia, R.M., Lastra-Ripoll, S.E., Mieleo-Gómez, L.D., García-Zapateiro, L.A., 2021. Physicochemical and rheological characterization of melon pulp (*Cucumis melo*) cultivated in the north of bolívar department, Colombia. Int. J. Adv. Sci., Eng. Inf. Technol. 11 (1), 185–190. <https://doi.org/10.18517/IJASEIT.11.1.7620>.
- Marsiglia-Fuentes, R., Quintana, S.E., García Zapateiro, L.A., 2022. Novel hydrocolloids obtained from mango (*Mangifera indica*) var. Hilaza: chemical, physicochemical, techno-functional, and structural characteristics. Gels 2022 Vol. 8, 354. <https://doi.org/10.3390/GELS8060354>.
- Martínez, K.D., Baeza, R.I., Millán, F., Pilosof, A.M.R., 2005. Effect of limited hydrolysis of sunflower protein on the interactions with polysaccharides in foams. Food Hydrocoll. 19 (3), 361–369. <https://doi.org/10.1016/J.FOODHYD.2004.10.002>.
- Martínez, M., Beltrán, O., Rincón, F., León De Pinto, G., Igartuburu, J.M., 2015. New structural features of *Acacia tortuosa* gum exudate. Food Chem. 182, 105–110. <https://doi.org/10.1016/J.FOODCHEM.2015.02.124>.
- Martínez, S.E.Q., Fuentes, E.E.T., Zapateiro, L.A.G., 2021. Food hydrocolloids from butternut squash (*Cucurbita moschata*) peel: rheological properties and their use in Carica papaya Jam. ACS Omega 6 (18), 12114. <https://doi.org/10.1021/ACSEOMEGA.1C00822>.
- Mata-Miranda, M.M., Guerrero-Robles, C.I., Rojas-López, M., Delgado-Macuil, R.J., González-Díaz, C.A., Sánchez-Monroy, V., Pérez-Ishiwara, D.G., Vázquez-Zapién, G.J., Mata-Miranda, M.M., Guerrero-Robles, C.I., Rojas-López, M., Delgado-Macuil, R.J., González-Díaz, C.A., Sánchez-Monroy, V., Pérez-Ishiwara, D.G., Vázquez-Zapién, G.J., 2017. Componentes Principales mediante Espectroscopia FTIR como Técnica de Caracterización Innovadora durante la Diferenciación de Células Madre Pluripotentes a Células Pancreáticas. Rev. Mex. De Ing. fa Biom. édicca 38 (1), 225–234. <https://doi.org/10.17488/RMIB.38.1.17>.
- Morris, E.R., 1990. Shear-thinning of 'random coil' polysaccharides: characterisation by two parameters from a simple linear plot. Carbohydr. Polym. 13 (1), 85–96. [https://doi.org/10.1016/0144-8617\(90\)90053-U](https://doi.org/10.1016/0144-8617(90)90053-U).
- Naji-Tabasi, S., Razavi, S.M.A., 2016. New studies on basil (*Ocimum basilicum* L.) seed gum: Part II—Emulsifying and foaming characterization. Carbohydr. Polym. 149, 140–150. <https://doi.org/10.1016/J.CARBPO.2016.04.088>.
- Naji-Tabasi, S., Razavi, S.M.A., 2017. Functional properties and applications of basil seed gum: an overview. Food Hydrocoll. 73, 313–325. <https://doi.org/10.1016/J.FOODHYD.2017.07.007>.
- Pal, S., Mal, D., Singh, R.P., 2005. Cationic starch: an effective flocculating agent. Carbohydr. Polym. 59 (4), 417–423. <https://doi.org/10.1016/J.CARBPO.2004.06.047>.
- Pamies, R., Hernández Cifre, J.G., del Carmen López Martínez, M., García de la Torre, J., 2008. Determination of intrinsic viscosities of macromolecules and nanoparticles. Comparison of single-point and dilution procedures. Colloid Polym. Sci. 286 (11), 1223–1231. <https://doi.org/10.1007/S00396-008-1902-2/FIGURES/3>.
- Pereira, C.T.M., Pereira, D.M., de Medeiros, A.C., Hiramatsu, E.Y., Ventura, M.B., Bolini, H.M.A., 2021. Skyr yogurt with mango pulp, fructooligosaccharide and natural sweeteners: Physical aspects and drivers of liking. LWT 150, 112054. <https://doi.org/10.1016/J.LWT.2021.112054>.
- Petrucchi, R.H., Herring, F.G., Madura, J.D.(2017). Química general. 1440.11a. ed. Phillips, G., Williams, P.(2009). Handbook of hydrocolloids. (<https://books.google.com/books?hl=es&lr=&id=3k-kAgAAQBAJ&oi=fnd&pg=PP1&ots=e6GaubPvLg&ig=m6xA7wspL3n88Y0pGdG0nE7n6j1>).
- Picout, D.R., Ross-Murphy, S.B.(2007). On the Mark-Houwink parameters for galactomannans(<https://doi.org/10.1016/j.carbpol.2007.03.010>).
- Pirsa, S., Hafezi, K., 2023. Hydrocolloids: structure, preparation method, and application in food industry. Food Chem. 399, 133967. <https://doi.org/10.1016/J.FOODCHEM.2022.133967>.
- Pourfarzad, A., Yousefi, A., Ako, K., 2021. Steady/dynamic rheological characterization and FTIR study on wheat starch-sage seed gum blends. Food Hydrocoll. 111, 106380. <https://doi.org/10.1016/J.FOODHYD.2020.106380>.
- Punia Bangar, S., Kumar, M., Whiteside, W.S., 2021. Mango seed starch: a sustainable and eco-friendly alternative to increasing industrial requirements. Int. J. Biol. Macromol. 183, 1807–1817. <https://doi.org/10.1016/J.IJBIOMAC.2021.05.157>.
- Rafe, A., Razavi, S.M.A., 2013. Dynamic viscoelastic study on the gelation of basil seed gum. Int. J. Food Sci. Technol. 48 (3), 556–563. <https://doi.org/10.1111/J.1365-2621.2012.03221.X>.
- Rayo, L.M., Chaguri e Carvalho, L., Sardá, F.A.H., Dacanal, G.C., Menezes, E.W., Tadini, C.C., 2015. Production of instant green banana flour (*Musa cavendishii*, var. Nanicão) by a pulsed-fluidized bed agglomeration. LWT - Food Sci. Technol. 63 (1), 461–469. <https://doi.org/10.1016/J.LWT.2015.03.059>.
- Razavi, S.M.A., Cui, S.W., Guo, Q., Ding, H., 2014. Some physicochemical properties of sage (*Salvia macrosiphon*) seedgum. Food Hydrocoll. 35, 453–462. <https://doi.org/10.1016/J.FOODHYD.2013.06.022>.
- Razmkhah, S., Razavi, S.M.A., Mohammadifar, M.A., 2016. Purification of cress seed (*Lepidium sativum*) gum: a comprehensive rheological study. Food Hydrocoll. 61, 358–368. <https://doi.org/10.1016/J.FOODHYD.2016.05.035>.
- Reaz, A.H., Abedin, M.J., Mohammad Abdullah, A.T., Satter, M.A., Farzana, T., 2023. Physicochemical and structural impact of CMC-hydrocolloids on the development of gluten-free foxtail millet biscuits. Heliyon 9 (6), e17176. <https://doi.org/10.1016/J.HELIYON.2023.E17176>.
- Rojas-Martin, L., Quintana, S.E., García-Zapateiro, L.A., 2023. Physicochemical, rheological, and microstructural properties of low-fat mayonnaise manufactured with hydrocolloids from *dioscorea rotundata* as a fat substitute. Processes 2023 Vol. 11, 492. <https://doi.org/10.3390/PR11020492>.
- Rojas-torres, S.A., Quintana, S.E., García-zapateiro, L.A., 2021. Natural yogurt stabilized with hydrocolloids from butternut squash (*Cucurbita moschata*) seeds: effect on physicochemical, rheological properties and sensory perception. Fluids 2021 6 (7), 251. <https://doi.org/10.3390/FLUIDS6070251>.
- Salvador, A., Fiszman, S.M., 1998. Textural characteristics and dynamic oscillatory rheology of maturation of milk gelatin gels with low acidity. J. Dairy Sci. 81 (6), 1525–1531. [https://doi.org/10.3168/JDS.S0022-0302\(98\)75718-2](https://doi.org/10.3168/JDS.S0022-0302(98)75718-2).

- Sánchez-González, L., Vargas, M., González-Martínez, C., Chiralt, A., Cháfer, M., 2009. Characterization of edible films based on hydroxypropylmethylcellulose and tea tree essential oil. *Food Hydrocoll.* 23 (8), 2102–2109. <https://doi.org/10.1016/J.FOODHYD.2009.05.006>.
- Vergara-Valencia, N., Granados-Pérez, E., Agama-Acevedo, E., Tovar, J., Ruales, J., Bello-Pérez, L.A., 2007. Fibre concentrate from mango fruit: characterization, associated antioxidant capacity and application as a bakery product ingredient. *LWT - Food Sci. Technol.* 40 (4), 722–729. <https://doi.org/10.1016/J.LWT.2006.02.028>.
- Wang, L., Liu, H.M., Zhu, C.Y., Xie, A.J., Ma, B.J., Zhang, P.Z., 2019. Chinese quince seed gum: Flow behaviour, thixotropy and viscoelasticity. *Carbohydr. Polym.* 209, 230–238. <https://doi.org/10.1016/J.CARBPOL.2018.12.101>.
- Wang, Y., Selomulya, C., 2022. Food rheology applications of large amplitude oscillation shear (LAOS). *Trends Food Sci. Technol.* 127, 221–244. <https://doi.org/10.1016/J.TIFS.2022.05.018>.
- Wei, Y., Guo, Y., Li, R., Ma, A., Zhang, H., 2021. Rheological characterization of polysaccharide thickeners oriented for dysphagia management: carboxymethylated curdlan, konjac glucomannan and their mixtures compared to xanthan gum. *Food Hydrocoll.* 110 <https://doi.org/10.1016/J.FOODHYD.2020.106198>.
- Yu, Z.Y., Jiang, S.W., Cao, X.M., Jiang, S.T., Pan, L.J., 2016. Effect of high pressure homogenization (HPH) on the physical properties of taro (*Colocasia esculenta* (L.) Schott) pulp. *J. Food Eng.* 177, 1–8. <https://doi.org/10.1016/J.JFOODENG.2015.10.042>.
- Zhu, Y., Bhandari, B., Prakash, S., 2019. Tribo-rheology characteristics and microstructure of a protein solution with varying casein to whey protein ratios and addition of hydrocolloids. *Food Hydrocoll.* 89, 874–884. <https://doi.org/10.1016/J.FOODHYD.2018.12.005>.
- Zhu, H., Xu, L., Wang, J., Zhang, Z., Xu, X., Yang, K., Sun, P., Liao, X., Cai, M., 2023. Rheological behaviors of ethanol-fractional polysaccharides from *Dendrobium officinale* in aqueous solution: Effects of concentration, temperature, pH, and metal ions. *Food Hydrocoll.* 137, 108311 <https://doi.org/10.1016/J.FOODHYD.2022.108311>.